Beaming effect in *Fermi* blazars

裴致远

Guangzhou University

Co-with 樊军辉，杨江河，肖胡兵 & Denis Bastieri

First LHAASO Collaboration Conference, Guangzhou, 04/25/2021

Main conclusions

- The radio core-dominance parameters can be taken as a good indicator for the study of beaming effect in gamma-ray blazars.
- Our derived result on the gamma-ray Doppler factor suggest that the gamma-ray emission of blazars is strongly beamed.
- We predict that the blazars candidates of neutrino emitters are potentially strongly Doppler boosting sources.

Outline

1. Introduction;
2. Radio core dominance (just mentioned);
3. The gamma-ray Doppler factor;
4. Summary.

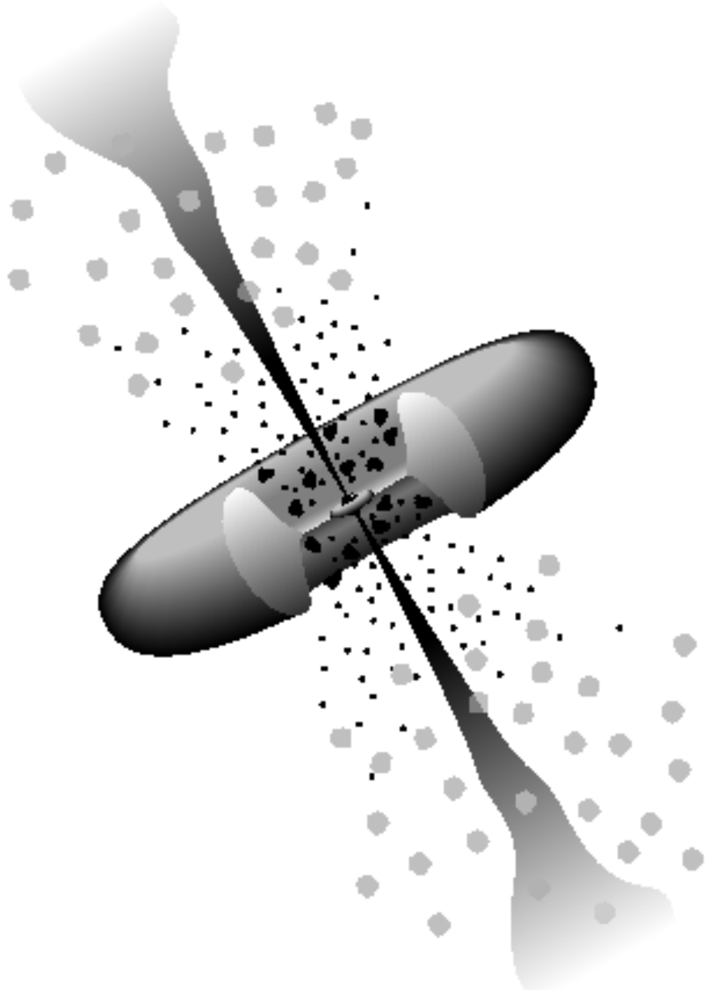

Outline

1. **Introduction;**
2. **Radio core dominance (just mentioned);**
3. **The gamma-ray Doppler factor;**
4. **Summary.**

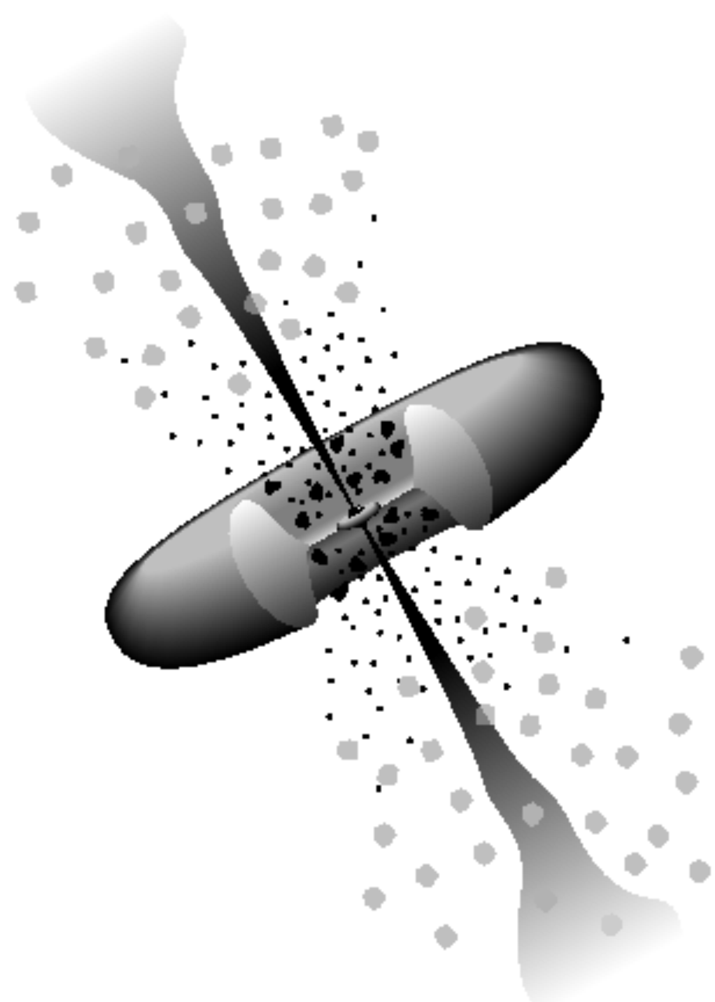

Standard model of AGNs

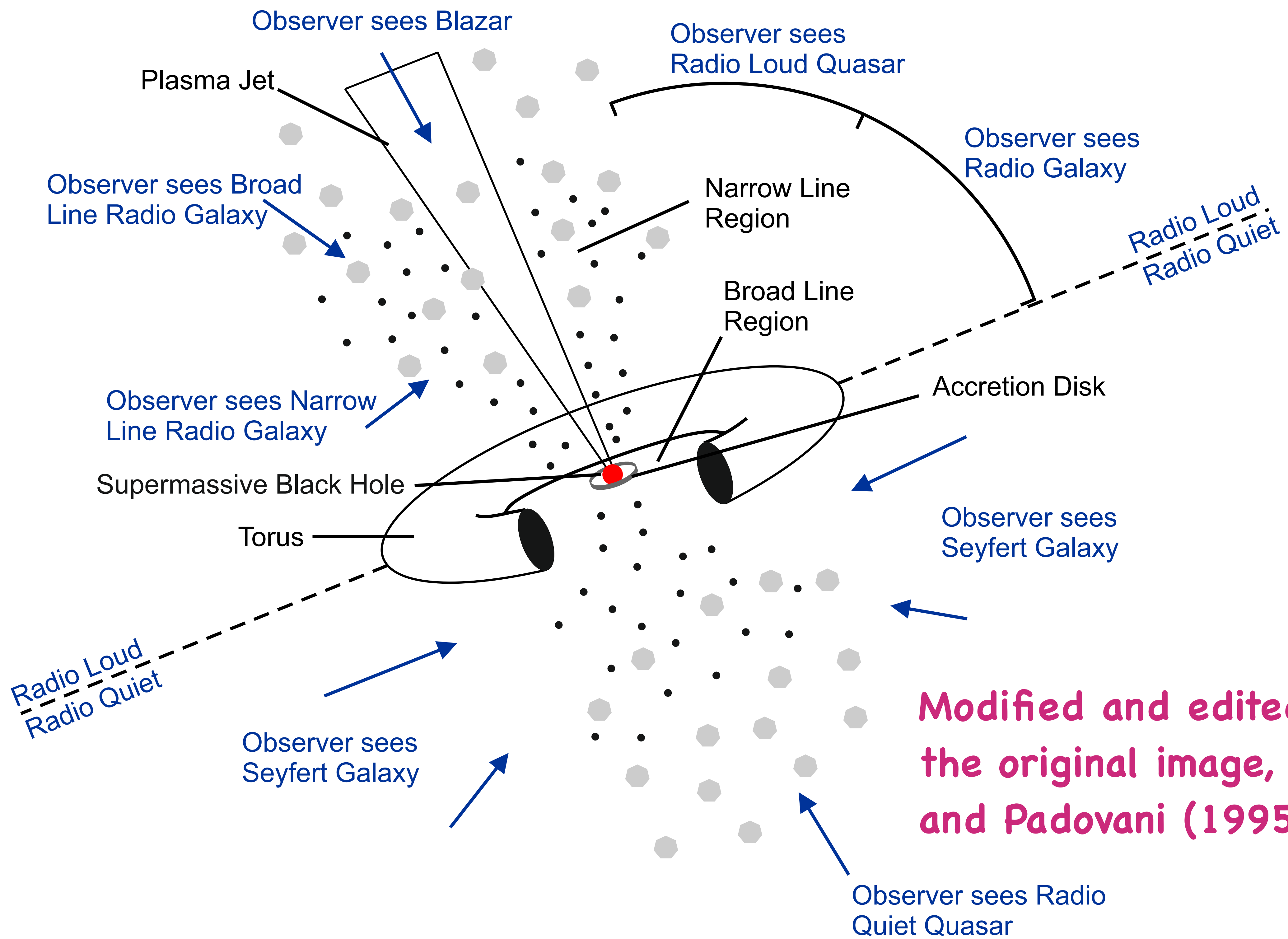

Modified and edited from the original image, see Urry and Padovani (1995, PASP)

Figure 1.1: Unification of AGN, not to scale. The viewing angle of the observer with respect to the jet axis determines what class of object is seen.

Blazars Characteristics

Illustration of the leptonic model for a typical blazar
Image credit: A. de Angelis

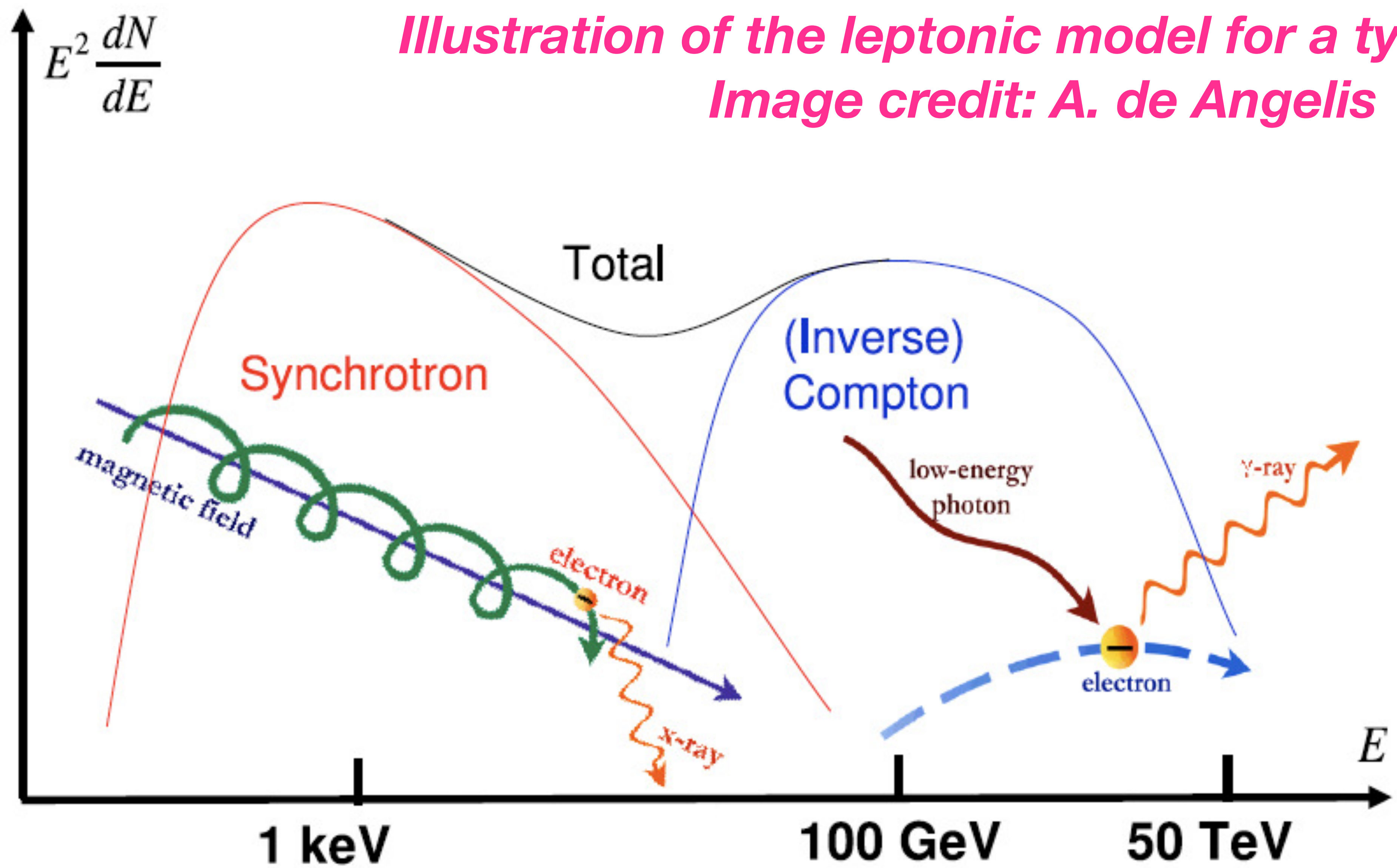

IC → **synchrotron self-Compton (SSC)** → **BL Lacs**

IC → **external inverse Compton (EC)** → **FSRQs**

Fermi-LAT Fourth Catalog (4FGL)

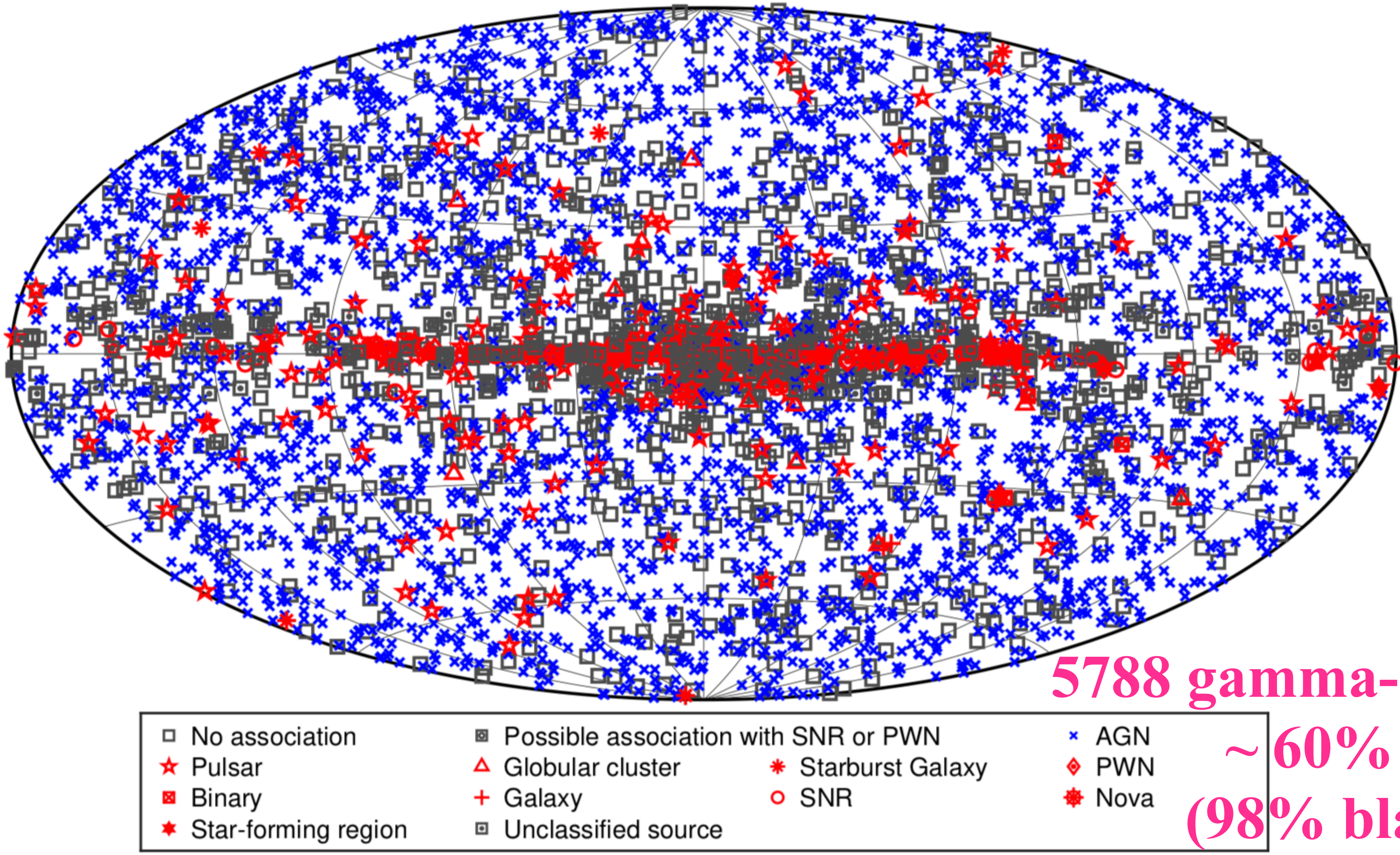

5788 gamma-ray objects
~ 60% AGN
(98% blazars)

(Imagecredit: Fermi-LAT collaboration)

Census of Sources in 4FGL

	Fourth catalog for Fermi Gamma-ray LAT (4FGL)	
Version	DR 1	DR 2
Energy Range	50 MeV-1 TeV	50 MeV-1 TeV
Duration	8 years	10 years
Sources	5064	5788 (+724)
Blazars	3137	3421 (+284)
BL Lacs	1132	1191 (+59)
FSRQs	694	733 (+39)
BCUs	1312	1498 (+186)

Census of Sources in 4FGL

	Fourth catalog for Fermi Gamma-ray LAT (4FGL)	
Version	DR 1	DR 2
Energy Range	50 MeV-1 TeV	50 MeV-1 TeV
Duration	8 years	10 years
Sources	5064	5788 (+724)
Blazars	3137	3421 (+284)
BL Lacs		
FSRQs		
BCUs		

DR 3 **are soon released (+248 blazars)**
Stay tuned!

Relativistic Beaming Effect

Doppler factor: $$\delta = \frac{1}{\Gamma(1-\beta\cos\phi)}$$

Lorentz factor: $$\Gamma = \frac{1}{1-\beta^2},\ \beta \equiv \frac{v}{c}$$

2+α for continuous jets
3+α for spherical blobs

$$S^{ob} = \delta^p S^{in}$$

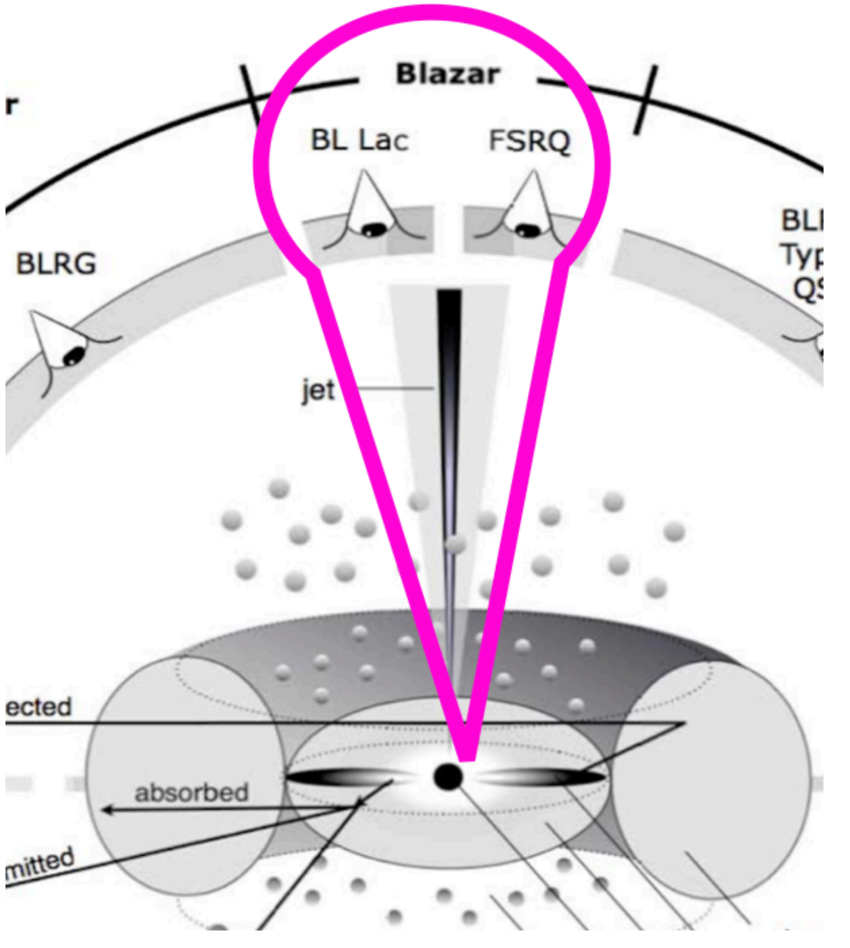

Scoring the Beaming!

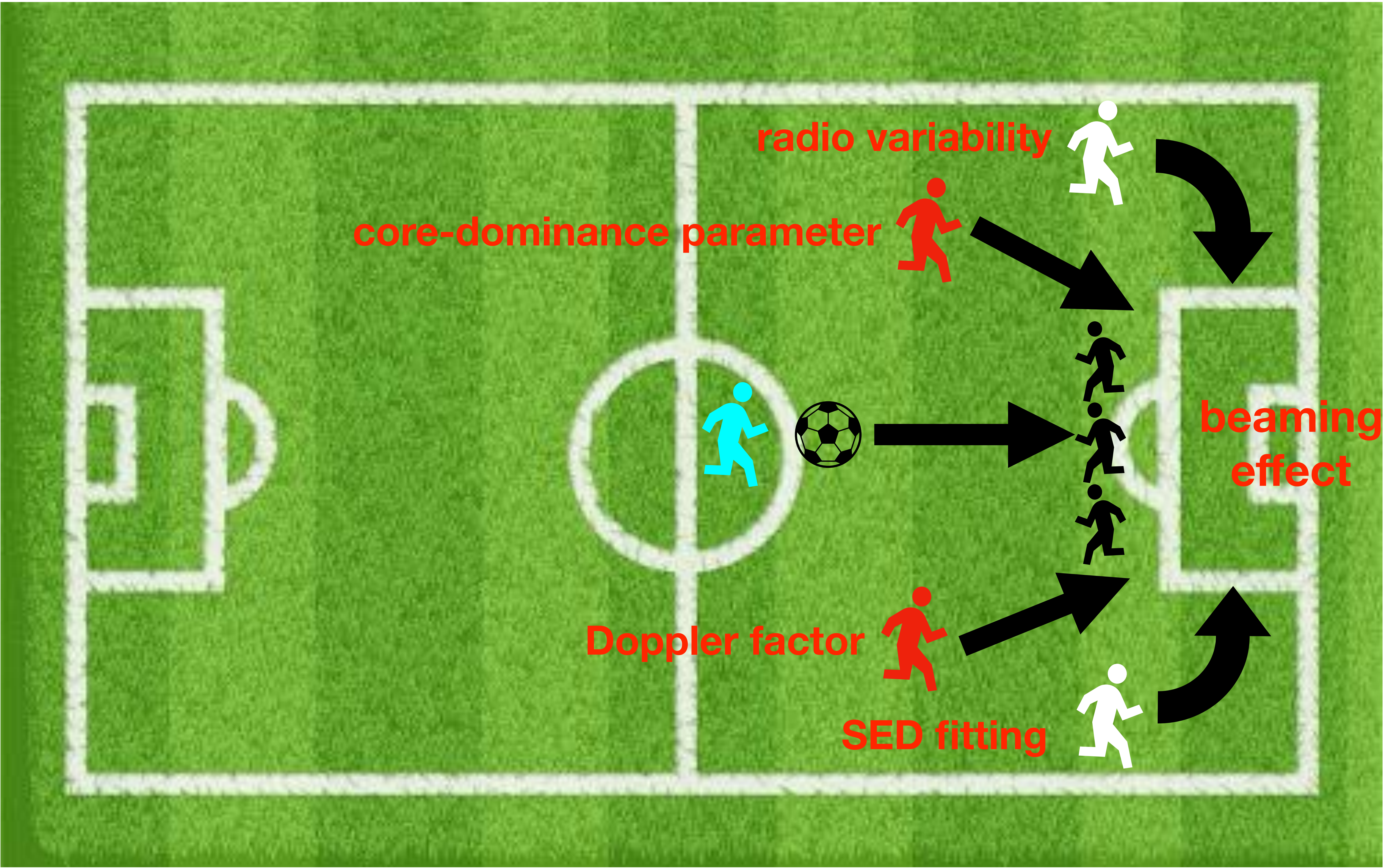

Outline

1. Introduction;
2. **Radio core dominance (just mentioned);**
3. The gamma-ray Doppler factor;
4. Summary.

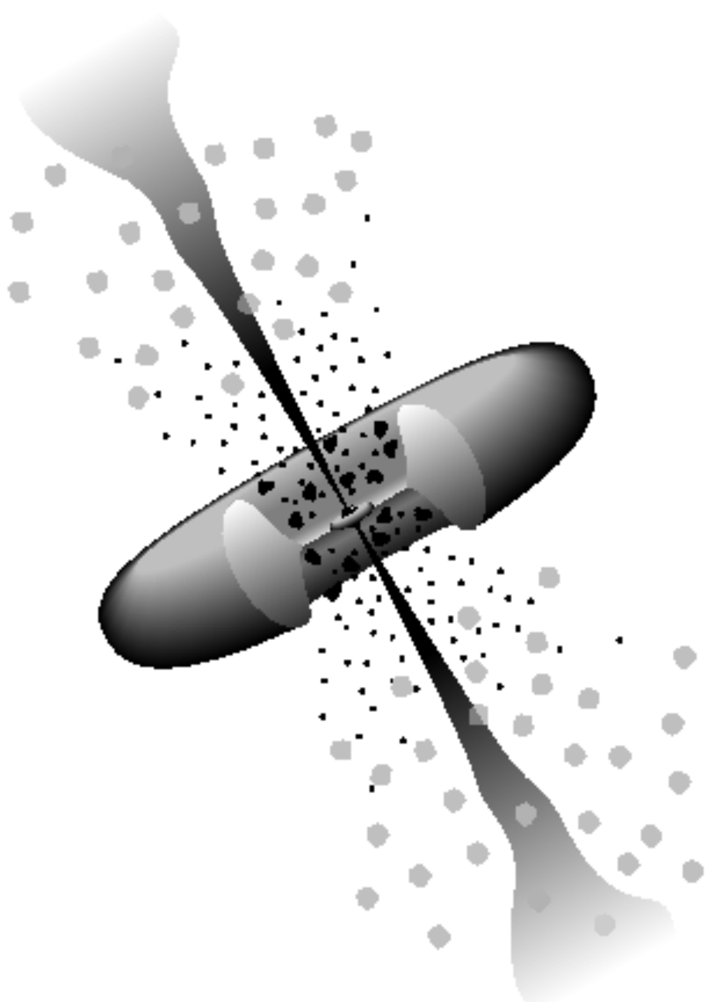

Radio core-dominance parameter

The radio emission is consisted of two components, namely the core and the extended emission.

$$R = \frac{S_{core}}{S_{extend}}$$

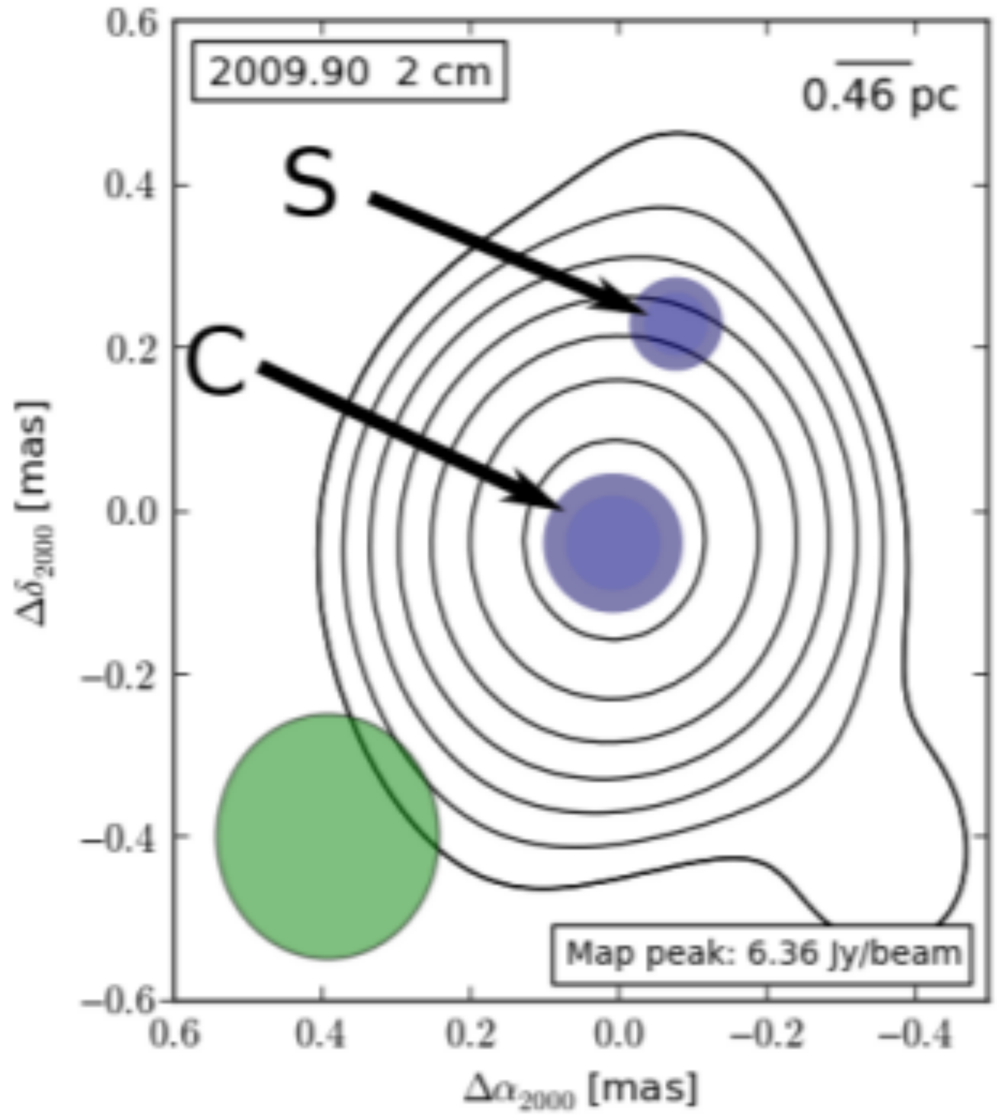

(Super-resolved VLBI maps of OJ 287 at 15 GHz)

Radio core-dominance parameter

We collected a largest catalog with available radio core-dominance parameters **(*log R*)**, up to **4388** sources. Based on 4FGL, we compiled **584 *Fermi blazars*** and **1310 *non-Fermi blazars*** with **log *R***. ***FBs*** consisted of **252 *BL Lacs*, 283 *FSRQs*** and **49 *BCUs***. We use these data to study the **beaming effect** and **radio dominance of** *Fermi* blazars.

The catalogues are available in VizieR:
http://vizier.u-strasbg.fr/viz-bin/VizieR?-source=VIII/108

(Pei+2020, SCPMA, 63, 259511;
see also Pei+2020, PASP, 132, 4102)

Comparison of logR between FBs and non-FBs

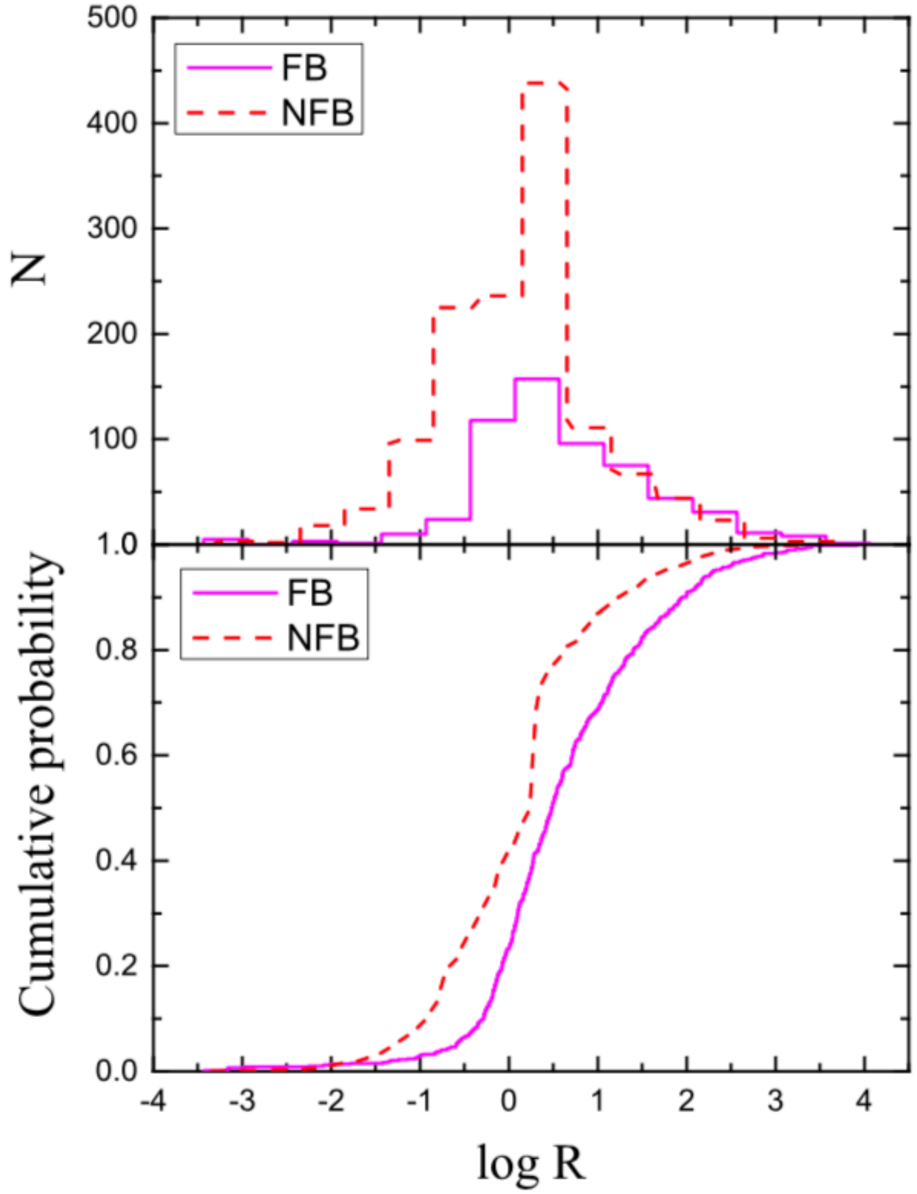

$$\text{FBs}: \langle \log \text{R} \rangle = 0.627 \pm 0.982$$

$$\text{non-FBs}: \langle \log \text{R} \rangle = 0.097 \pm 0.869$$

K-S test: $p = 3.428 \times 10^{-31}$

Figure 4 Distributions of the core-dominance parameters log *R* (upper panel) and the cumulative probabilities (lower panel) for the entire blazar sample. In this plot, the magenta solid line indicates the FBs and the red dashed line for NFBs.

Outline

1. Introduction;
2. Radio core dominance (just mentioned);
3. **The gamma-ray Doppler factor;**
4. Summary.

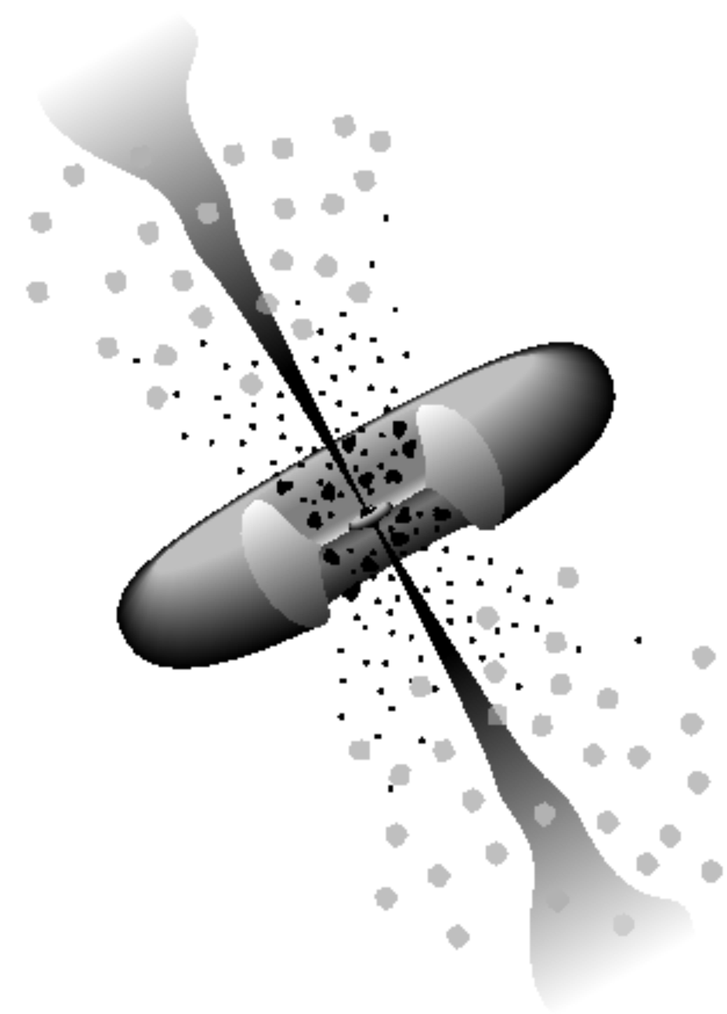

Gamma-ray Doppler factor

- Deduced by a synchrotron self-Compton (SSC) (δ_{ssc}, e.g., Ghisellini et al. 1993)
- Derived from adopting single-epoch radio data by assuming that the sources hold an equipartition of energy between radiating particles and magnetic field (δ_{eq}, e.g., Readhead 1994)
- Estimated using the radio flux density variations or brightness temperature denoted (δ_{var}, e.g., Lähteenmäki & Valtaoja 1999; Fan et al. 2009; Hovatta et al. 2009; Liodakis et al. 2018).
- Constrained from SEDs fitting model (e.g. Chen 2018).
- etc.

However, discrepancies exist!!

Methodology

In our work, some assumptions need to be taken into account (Mattox et al. 1993; Fan et al. 2013, 2014)

(1) X-ray is produced in the same region as γ-rays, and the intensities of X-ray and γ-ray are semblable when γ-ray emission is observed;

(2) the emission region is spherical;

(3) the emission is isotropic, and the size of the emission region is constrained by the time scale of variability, ΔT, to be less than $R_{size}=c\delta\Delta T/(1+z)$.

Methodology

then we derive the optical depth for the pair production expressed by

$$\tau = 2\times 10^{3}\left[\left(1+z\right)/\delta\right]^{4+2\alpha}\left(1+z-\sqrt{1+z}\right)^{2} h_{75}^{-2}\Delta T_{5}^{-1}\left(\frac{F_{1\mathrm{keV}}}{\mu\mathrm{Jy}}\right)\left(\frac{E_{\gamma}}{\mathrm{GeV}}\right)^{\alpha}$$

and considering the luminosity distance in the form of

$$d_{L} = \frac{c}{H_{0}}\int_{1}^{1+z}\frac{dx}{\sqrt{\Omega_{M}x^{3}+1-\Omega_{M}}},$$

thus the optical depth τ can be rewritten into

$$\tau = 1.54\times 10^{-3}\left(\frac{1+z}{\delta}\right)^{4+2\alpha}\left(\frac{d_{L}}{\mathrm{Mpc}}\right)^{2}\left(\frac{\Delta T}{\mathrm{h}}\right)^{-1}\left(\frac{F_{1\mathrm{kev}}}{\mu\mathrm{Jy}}\right)\left(\frac{E_{\gamma}}{\mathrm{GeV}}\right)^{\alpha}$$

Methodology

Therefore, the lower limit on γ-ray Doppler factor can be estimated if we assume the optical depth dose not exceed unity (Mattox et al. 1993; Fan et al. 2013, 14)

$$\delta_\gamma \geq \left[1.54\times10^{-3}(1+z)^{4+2\alpha}\left(\frac{d_L}{\mathrm{Mpc}}\right)\left(\frac{\Delta T}{\mathrm{h}}\right)^{-1}\left(\frac{F_{\mathrm{1kev}}}{\mu\mathrm{Jy}}\right)\left(\frac{E_\gamma}{\mathrm{GeV}}\right)^{\alpha}\right]^{\frac{1}{4+2\alpha}}$$

(Pei+2020, PASA, 37, 43)

Sample

Overall 809 blazars (342 FSRQs+467 BL Lacs)

Table 1. The lower limit on γ-ray Doppler factor for *Fermi* blazars

4FGL Name	Other Name	Class	z	$\log R$	$F_{1\,\mathrm{keV}}$	α_X	Ref.	$\alpha_\gamma^{\mathrm{ph}}$	E_γ	L_X	L_γ	δ_γ	δ_{L18}	δ_{C18}
(1)	(2)	(3)	(4)	(5)	(6)	(7)	(8)	(9)	(10)	(11)	(12)	(13)	(14)	(15)
J0005.9 + 3824	0003 + 380	FSRQ	0.229	1.13	0.080	1.32	Y19	2.67	2.39	43.44	44.46	1.92	5.23	5.6
J0006.3 − 0620	0003 − 066	HBL	0.347	0.26	0.152		NED	2.17	3.75	44.14	44.48	2.95	6.96	
J0010.6 + 2043	0007 + 205	FSRQ	0.6	0.29	0.058		NED	2.32	3.20	44.30	45.12	3.56	6.02	
J0019.6 + 7327	0016 + 731	FSRQ	1.781	0.54	0.015		NED	2.59	2.51	44.88	47.30	6.96	7.84	
J0050.7 − 0929	0048 − 097	IBL	0.634	1.20	0.392	1.57	Y19	2.04	4.41	45.19	46.64	5.12	20.23	28.4
J0108.6 + 0134	0106 + 013	FSRQ	2.099	0.71	0.065	0.43	Y19	2.35	3.08	45.69	48.37	14.45	2.64	15.3
J0113.4 + 4948	0110 + 495	FSRQ	0.389	0.98	0.104	2.24								
J0116.0 − 1136	0113 − 118	FSRQ	0.670	1.02	0.180	0.98								
J0132.7 − 1654	0130 − 171	FSRQ	1.020	0.36	0.034									
J0137.0 + 4751	0133 + 476	FSRQ	0.859	0.91	0.324	0.82								
J0141.4 − 0928	0138 − 097	IBL	0.733	−0.04	0.045	1.15								
J0152.2 + 2206	0149 + 218	FSRQ	1.320	0.69	0.048									
...	...	...	...	...	...	...								

Note: Col. 1 gives 4FGL name; Col. 2 counterpart name; Col. 3 classification (FSRQ intermediate synchrotron peak BL Lacs; LBL: low synchrotron peak BL Lacs); Col. 4 r units of μJy at 1 keV; Col. 7 X-ray spectral index; Col. 8 Reference for Col. 6 and 7 (Y1 Roma BZCAT- 5th edition, Multi-frequency Catalogue of Blazars); Col. 9 γ-ray photon luminosity in units of erg s^{-1} Col. 12 γ-ray luminosity in units of erg s^{-1}; Col. 13 the d factor from Liodakis et al. (2018); Col. 15 the estimated Doppler factor from Chen (2

507 sources with radio core dominance parameters (Pei+2020)

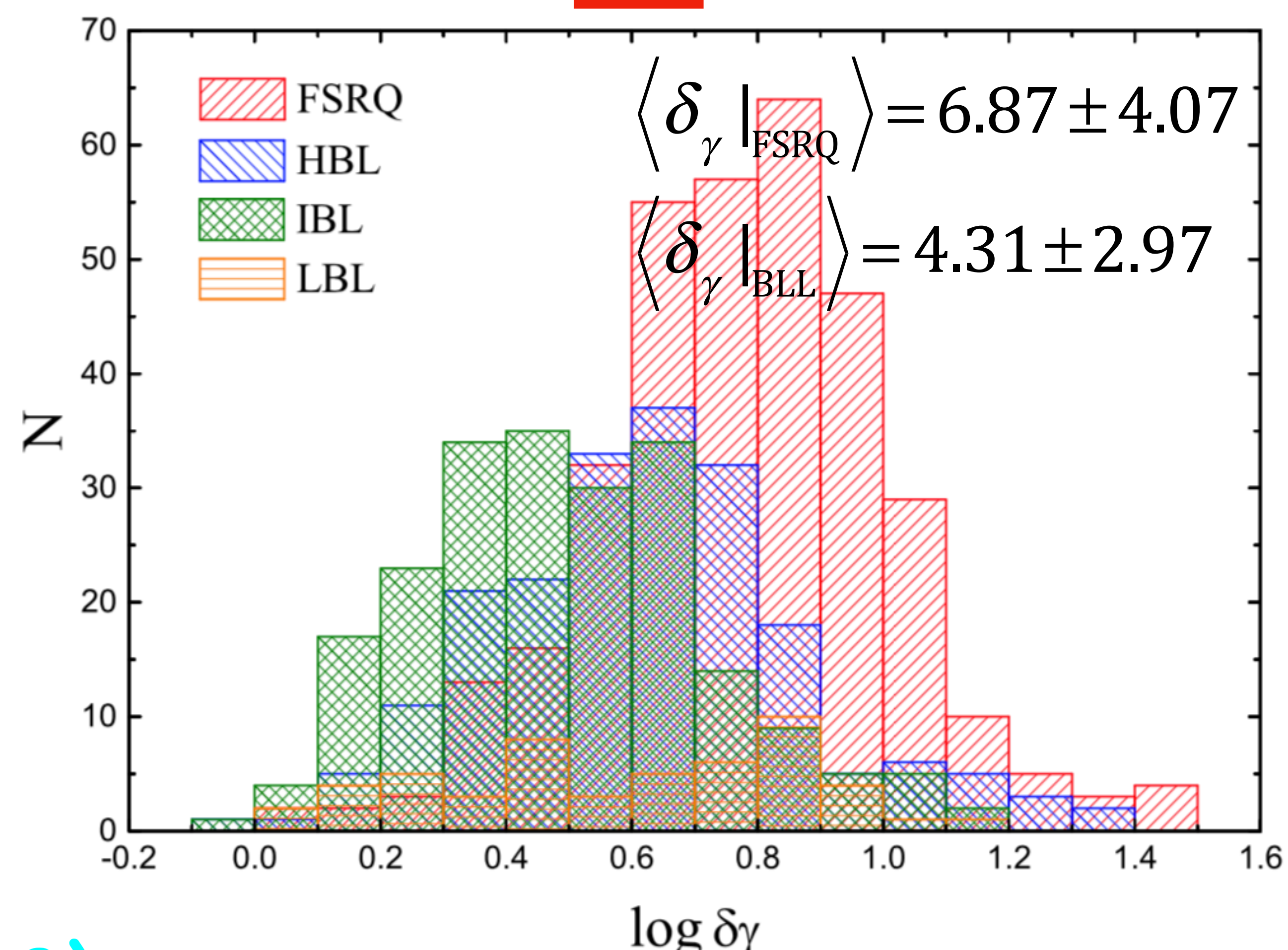

Fig. 1. Distributions of the γ-ray Doppler factor (δ_γ) in logarithm.

Discussion (I)

alternative assumption (i)

$\Delta T = 6$ hs

$$\delta_\gamma^{6hs} \sim 1.32\,\delta_\gamma^{24hs}$$

$\Delta T = 48$ hs

$$\delta_\gamma^{48hs} \sim 0.87\,\delta_\gamma^{24hs}$$

alternative assumption (ii)

$$\delta_{\text{continuous}} = \delta_{\text{sphere}}^{(4+2\alpha)/(3+2\alpha)}$$

(Ghisellini et al. 1993)

$$\log \delta_\gamma^{2+\alpha} \sim 1.14 \log \delta_\gamma^{3+\alpha}$$

(This work)

Discussion (II)

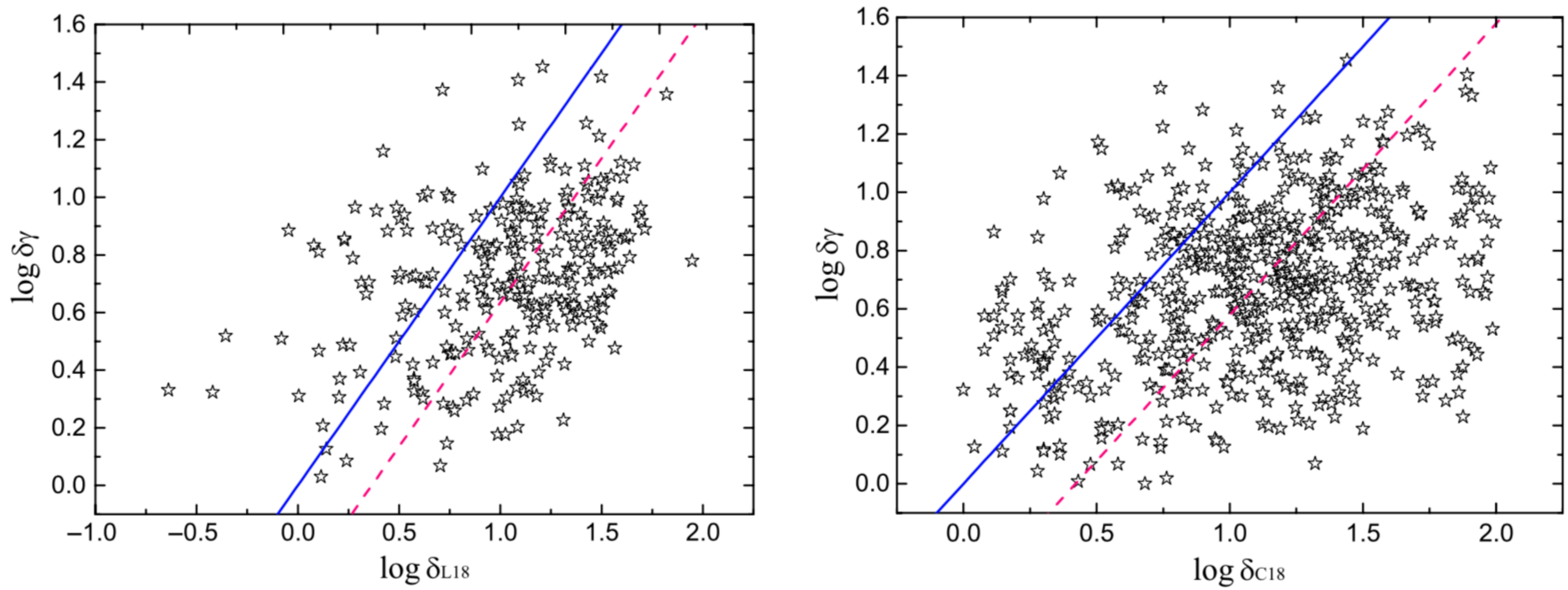

Figure 2. Plot of the correlation between log δ_γ derived in this paper and that presented from other literature after cross-checking. log δ_{L18} denotes the variability Doppler factor adopted from Liodakis et al. (2018) (left panel) and log δ_{C18} denotes the SED fitting derived Doppler factor from Chen (2018) (right panel). The solid blue lines refer to the equality line and the dashed pink ones signify the half proportion dividing line that are parallel to the equality one.

Discussion (II)

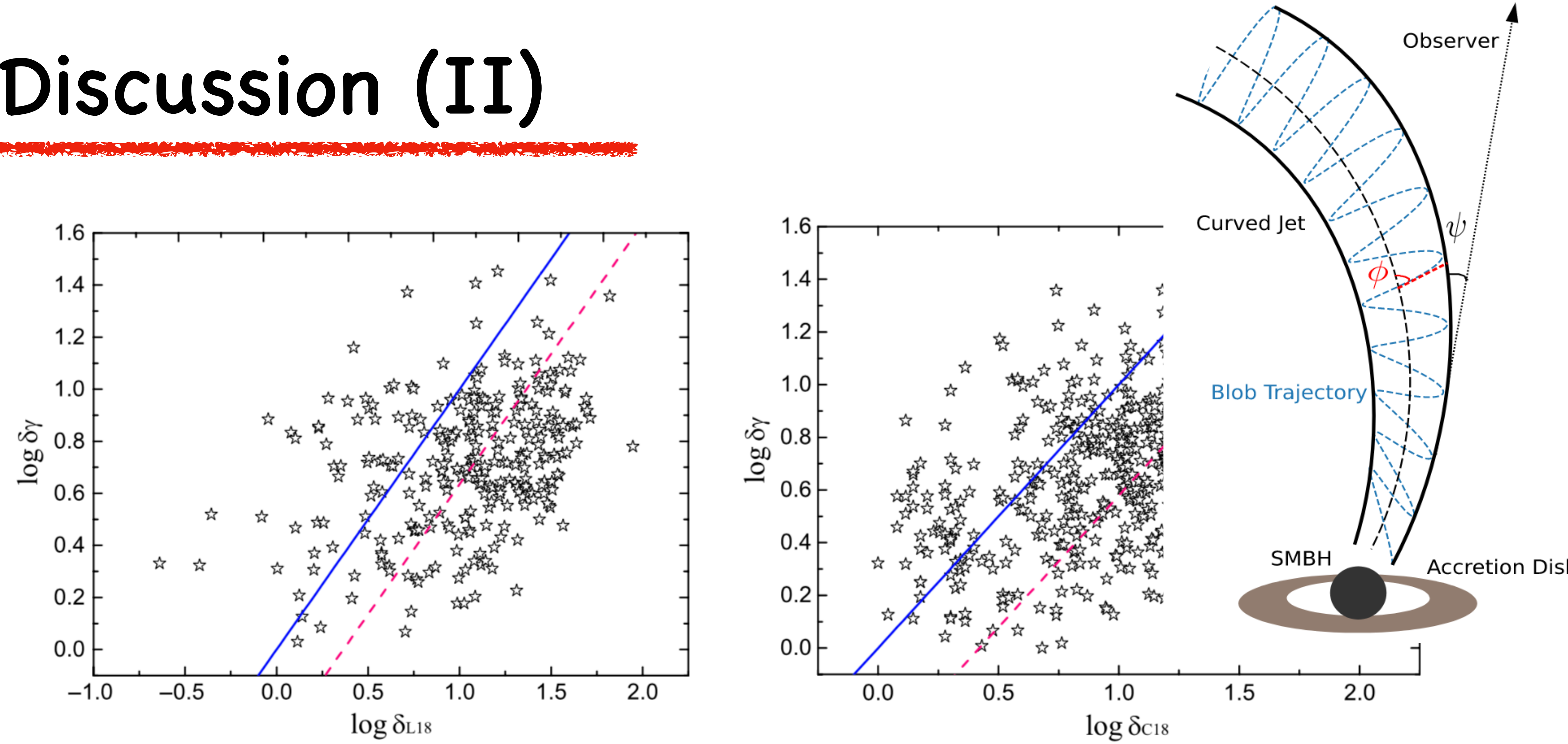

Figure 2. Plot of the correlation between log δ_γ derived in this paper and that presented from other literature after cross-checking. log δ_{L18} denotes the variability Doppler factor adopted from Liodakis et al. (2018) (left panel) and log δ_{C18} denotes the SED fitting derived Doppler factor from Chen (2018) (right panel). The solid blue lines refer to the equality line and the dashed pink ones signify the half proportion dividing line that are parallel to the equality one.

Implication:

(i) **Jet bending:** If a bend in the jet takes place at upstream of the γ-ray emission region and downstream of extended radio-emitting region, probably resulting in a γ-ray-loud but radio-quiet AGN.

Discussion (II)

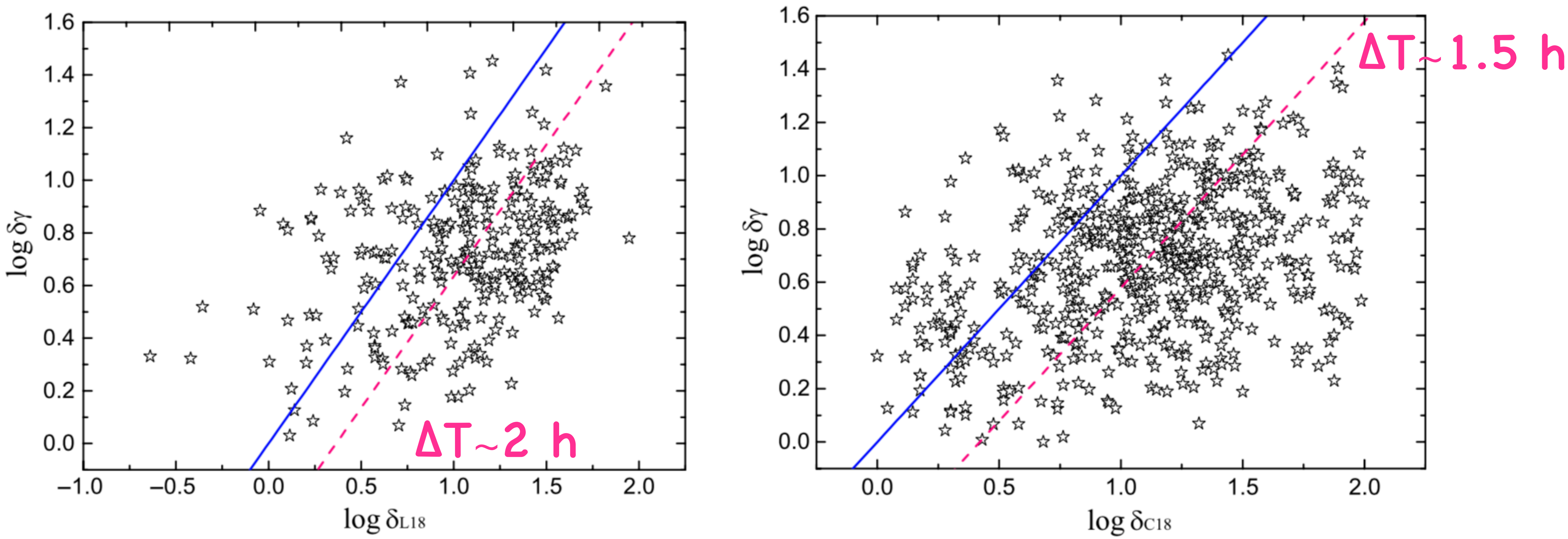

Figure 2. Plot of the correlation between log δ_γ derived in this paper and that presented from other literature after cross-checking. log $\delta_{\rm L18}$ denotes the variability Doppler factor adopted from Liodakis et al. (2018) (left panel) and log $\delta_{\rm C18}$ denotes the SED fitting derived Doppler factor from Chen (2018) (right panel). The solid blue lines refer to the equality line and the dashed pink ones signify the half proportion dividing line that are parallel to the equality one.

Implication:

(ii) **Variability timescale:** Suggesting that the on average, variability timescale for Fermi-detected blazars is around 1.5~2h; however, we cannot reach firm conclusions.

Discussion (III)

The γ-ray Doppler factor of neutrino emitter candidates are relatively quite high, suggesting these sources are also possibly strongly Doppler-boosted, e.g.

- TXS 0506+056 (4FGL J0509.4+0542), we report δ_γ=4.25
- PKS 1502+106 (4FGL J1504.4+1092), We derive δ_γ=13.41. For comparison, Chen (2018) obtained δ=23.80 and 13.77 for Liodakis et al. (2018).
- RXJ1022.7-0112 (4FGL J1022.7-0112), we have δ_γ=21.22.
- TXS 0628-240 (4FGL J0630.9-2406), δ_γ=10.43 are reported in our work. Chen (2018) has shown δ=51!
- PKS B1424-418 (4FGL J1427.9-4206), a PeV neutrino candidate, δ_γ=11.40 are obtained in our paper.

(Pei+2020, PASA, 37, 43)

Outline

1. Introduction;
2. Radio core dominance (just mentioned);
3. The gamma-ray Doppler factor;
4. **Summary.**

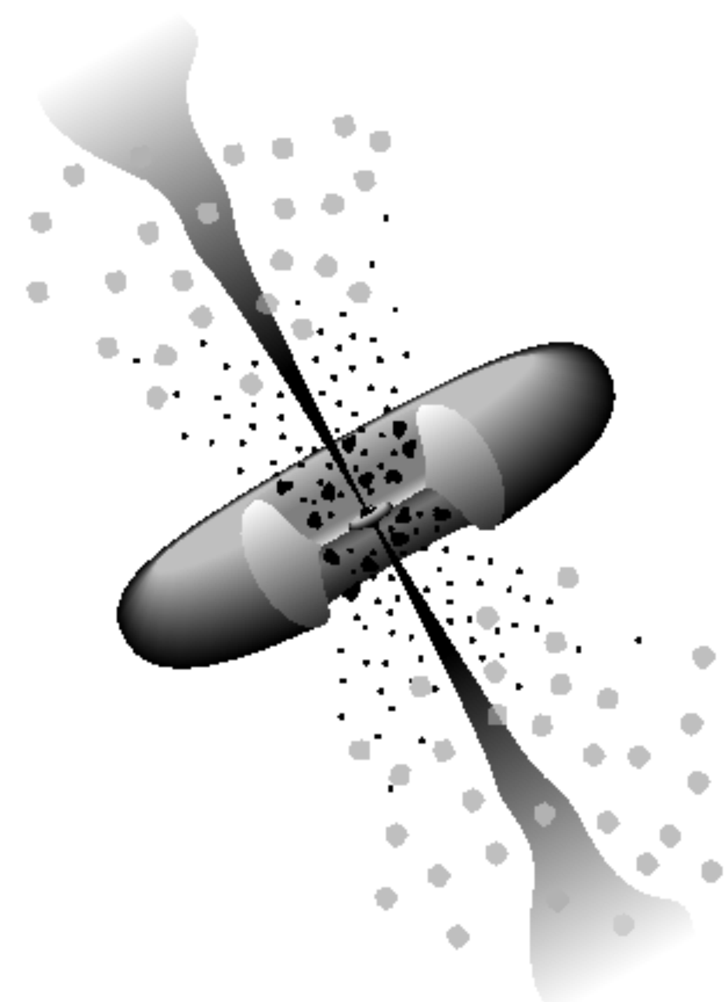

Conclusions

- The radio core-dominance parameters can be taken as a good indicator for the study of beaming effect in gamma-ray blazars.
- Our derived result on the gamma-ray Doppler factor suggest that the gamma-ray emission of blazars is strongly beamed.
- We predict that the blazars candidates of neutrino emitters are potentially strongly Doppler boosting sources.
- The estimation on the gamma-ray Doppler factor are higher than that from the radio band is believed to be due to the jet bending in those blazars.

LOC Announcement

18:30, tonight

Thank you for your attention!

谢谢！